Virchows Archiv A Pathol Anat (1993) 422:225–231

Virchows Archiv A
Pathological Anatomy and Histopathology

Localized amyloidosis in squamous cell carcinoma of uterine cervix: electron microscopic features of nodular and star-like amyloid deposits

Toshikazu Gondo[1], Tokuhiro Ishihara[1], Hiroo Kawano[1], Fumiya Uchino[1], Mutsuo Takahashi[2], Takako Iwata[3], Noboru Matsumoto[3], Tadaaki Yokota[4]

[1] The First Department of Pathology, Yamaguchi University School of Medicine, Ube, Yamaguchi 755, Japan
[2] Department of Clinical Laboratories, Yamaguchi University School of Medicine, Ube, Yamaguchi, Japan
[3] The School of Allied Health Science, Yamaguchi University, Ube, Yamaguchi, Japan
[4] Department of Pathology, Kokura Memorial Hospital, Kitakyushu, Fukuoka, Japan

Received September 1, 1992 / Received after revision October 8, 1992 / Accepted October 9, 1992

Abstract. An ultrastructural study of amyloid deposits in four cases of squamous cell carcinoma of uterine cervix was performed. The amyloid deposits reacted with anti-keratin antiserum on frozen sections. Amyloid deposits showed nodular (4 cases) and star-like forms (3 cases). Nodular amyloid deposits were composed of slightly whorled fibrils, measuring 7–10 nm in width. Some of them contained cellular debris and thicker, more electron-dense filaments than amyloid fibrils. In three cases, filamentous tumour cells and filamentous masses were observed together with amyloid. Star-like amyloid deposits were composed of bundles of straight amyloid fibrils. Some of the tumour cells in contact with star-like amyloid deposits had deep cytoplasmic invaginations, where closely packed amyloid fibrils were arrayed in parallel fasion. In addition, a few tumour cells had membrane-bound amyloid fibrils in the cytoplasm. It is suggested that nodular amyloid deposits are derived from the tumour cells through filamentous degeneration. Amyloid fibrils in star-like amyloid deposits are thought to be formed within the cytoplasm or in the vicinity of invaginated cytoplasmic membranes of the tumour cells.

Key words: Amyloid – Amyloidosis – Squamous cell carcinoma – Keratin – Ultrastructure

Introduction

Localized amyloidosis is frequently associated with neoplastic (Meyer 1968; Schober and Nelson 1975; Yamashita et al. 1985) and non-neoplastic lesions (Westermark and Grimelius 1973; Takahashi et al. 1986) in endocrine glands. In primary localized cutaneous amyloidosis, electron microscopic studies have demonstrated that amyloid deposits are derived from the epidermal keratinocytes through filamentous degeneration (Hashimoto and Kumakiri 1979; Kumakiri and Hashimoto 1979). It has been reported that these amyloid deposits have an identical antigenicity to epidermal keratin (Masu et al. 1981; Kobayashi and Hashimoto 1983). Localized amyloid deposits have been described in basal cell carcinoma (Malak and Smith 1962; Looi 1983), nasopharyngeal carcinoma (Prathap et al. 1984) and vaginal squamous cell carcinoma (Hsueh and Kuo 1986) and these deposits have been thought to be derived from the degenerating tumour cells. However, detailed investigations have not been performed on the ultrastructural features of the deposits.

We have examined the ultrastructural features of amyloid deposits in four cases of squamous cell carcinoma of the uterine cervix.

Correspondence to: T. Gondo

Materials and methods

The patients were 55, 59, 61 and 81 years old. The tumours were all invasive squamous cell carcinoma, large cell non-keratinizing type. No patients had history of radio or chemotherapy until biopsies and operations were performed.

Tumours were fixed in 10% formalin and embedded in paraffin. Sections were stained with haematoxylin and eosin and alkaline Congo red.

Immunohistochemically, amyloid deposits were examined for amyloid protein (Aκ, Aλ, AA, transthyretin) and keratin using antibodies for each antigen by the immunoperoxidase-antiperoxidase method. Production of antibodies against Aκ, Aλ and AA has been described, as has the characterization of these antisera (Fujihara et al. 1980). Antibodies against transthyretin and keratin were obtained from Dakopatts (Copenhagen, Denmark). The dilutions used were as follows: anti-Aκ, 1:4000; anti-Aλ, 1:8000; anti-AA, 1:500; anti-transthyretin, 1:500; anti-keratin, 1:500. Fresh frozen sections were available in one case. Tissues obtained from systemic amyloidosis patients served as positive controls, and sections of tissues run in parallel (except for replacement of the primary antisera by normal rabbit serum) served as negative controls.

For electron microscopic observations, small pieces of tumour tissue were fixed in 2.1% glutaraldehyde, post-fixed in 1% osmium tetroxide, dehydrated and embedded in Epon 812. Sections 1 μm thick were stained with toluidine blue to identify the lesion and confirm the presence of amyloid deposits. Thin sections were stained with uranyl acetate and lead citrate and examined by a Hitachi H-300 or H-800 electron microscope.

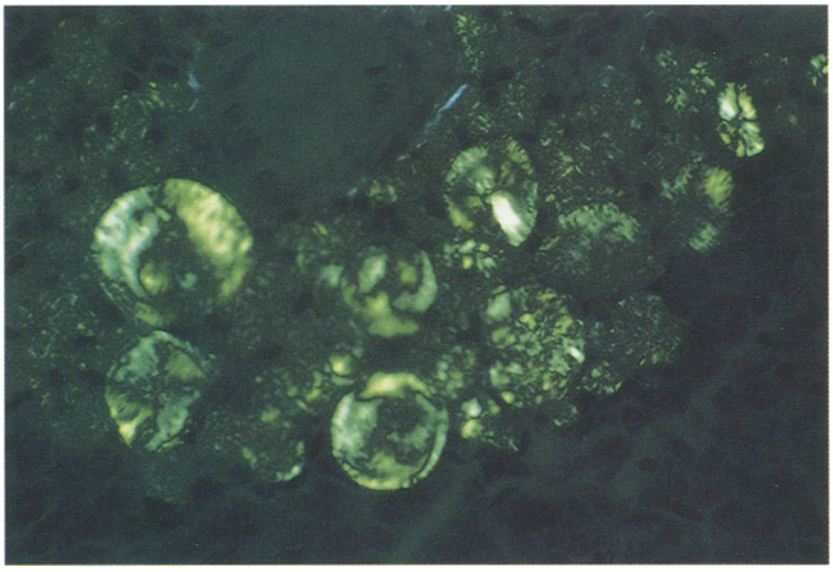

Fig. 1. Amyloid deposits show emerald-green birefringence. Congo red stain under polarized light

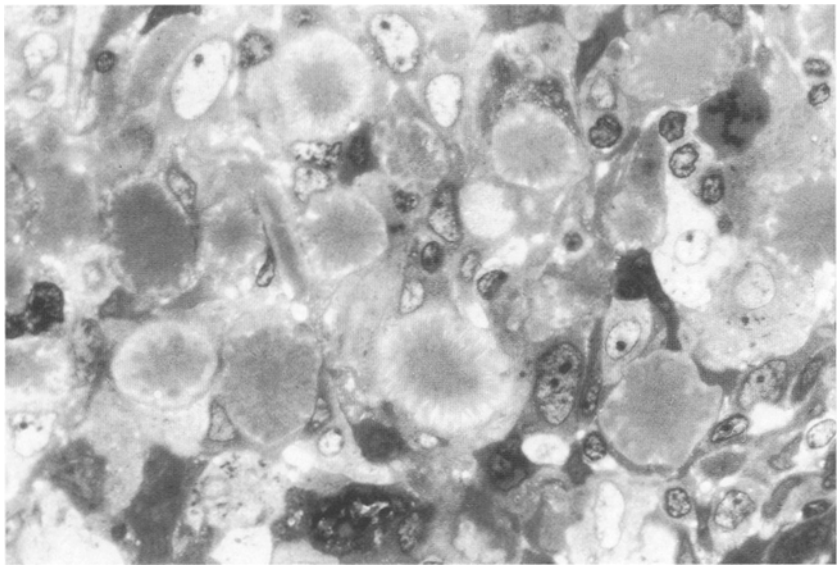

Fig. 2. Amyloid deposits showing amyloid star are located among tumour cells. Section 1 μm thick. Toluidine blue stain

Results

Light microscopically, there were varying amounts of eosinophilic material among the tumour cells and in the stroma. Most was in the form of nodules measuring about 10–30 μm in diameter. The deposits were stained orange-red with Congo red and showed emerald-green birefringence under polarized light (Fig. 1). In cases 1, 3 and 4, some of the deposits showed amyloid stars (Fig. 2).

These amyloid deposits did not react with anti-Aκ, Aλ, AA, transthyretin and keratin antisera on paraffin sections. However, the amyloid deposits were positive for anti-keratin antiserum on fresh frozen sections in case 1.

Ultrastructurally, the amyloid deposits exhibited nodular (Fig. 3) and star-like forms (Fig. 4) located close to tumour cells. Nodular amyloid deposits, noted in all four cases, were composed of slightly whorled amyloid fibrils, measuring 7–10 nm in width (Fig. 5). Some nodular amyloid deposits contained remnants of cellular debris (Fig. 5). In cases 2, 3 and 4, there were filamentous tumour cells and filamentous masses together with the amyloid deposits. The filamentous tumour cells, shrunken and detached from the neighbouring tumour cells (Fig. 6), contained a mass of whorled filaments which were less electron dense than tonofilaments. The filamentous masses were composed of whorled filaments without cytoplasmic membranes. These changes were morphologically identical to the filamentous degeneration of epidermal keratinocytes described in lichen planus and several other dermatoses (Hashimoto 1976) and primary localized cutaneous amyloidosis (Hashimoto and Kumakiri 1979; Kumakiri and Hashimoto 1979).

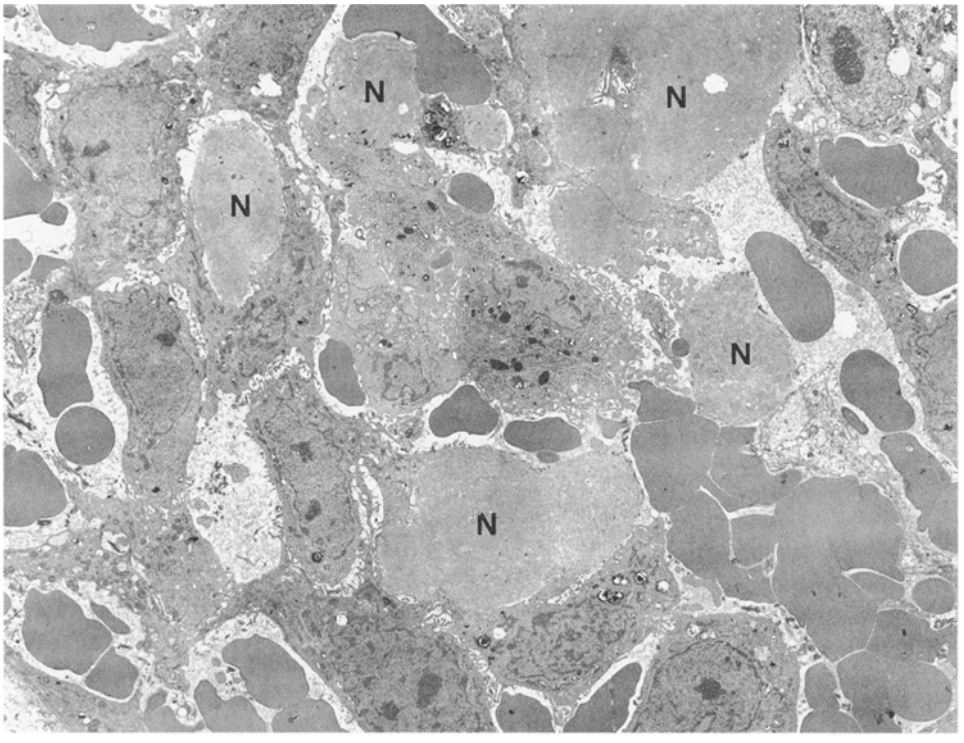

Fig. 3. Several nodular amyloid deposits (*N*) are scattered among tumour cells. ×2000

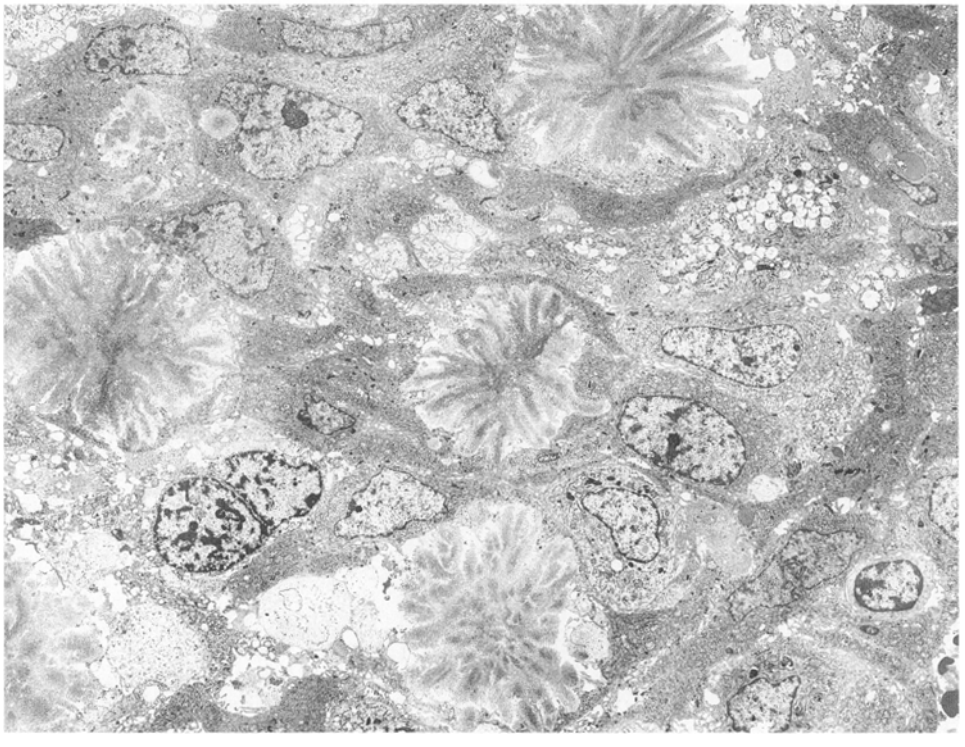

Fig. 4. Star-like amyloid deposits are composed of amyloid bundles. ×1700

In some nodular amyloid deposits, thicker and more electron-dense fibrils like tonofilaments were intermingled with amyloid fibrils (Fig. 7) and the former filaments were also contained in the filamentous tumour cells.

The star-like amyloid deposits, observed in cases 1, 3 and 4, were composed of bundles of straight amyloid fibrils (Fig. 8), measuring 7–10 nm in width, which formed felt-like structures in the centre of the deposits. Some of the tumour cells were in contact with these

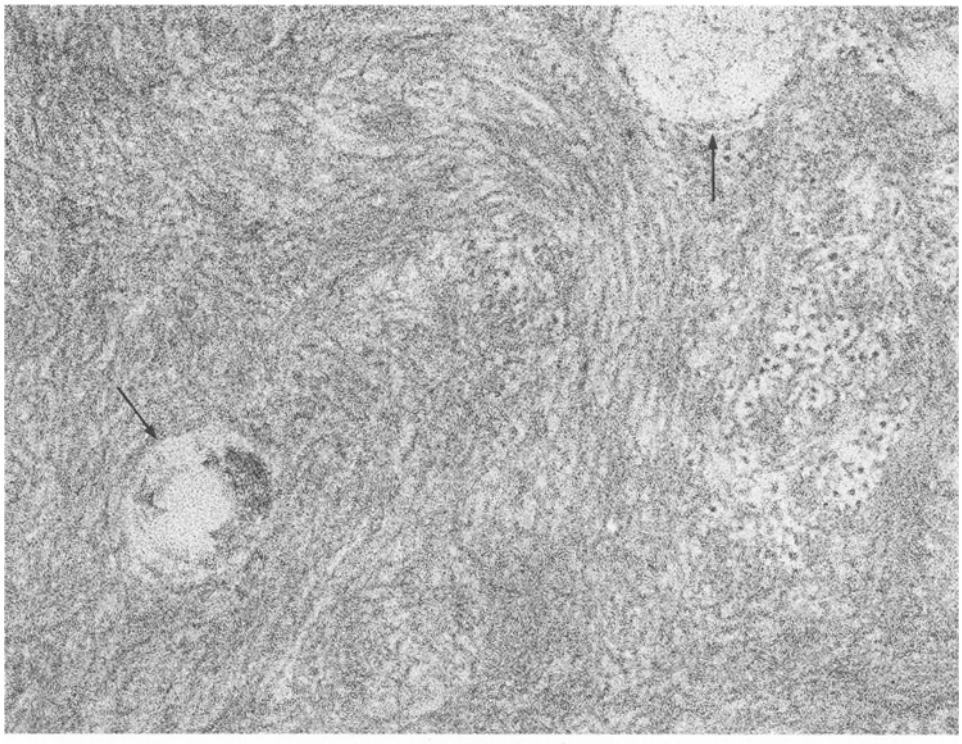

Fig. 5. A nodular deposit is composed of slightly whorled amyloid fibrils. A few remnants of the cellular debris (*arrows*) remain in the nodular amyloid deposit. ×100000

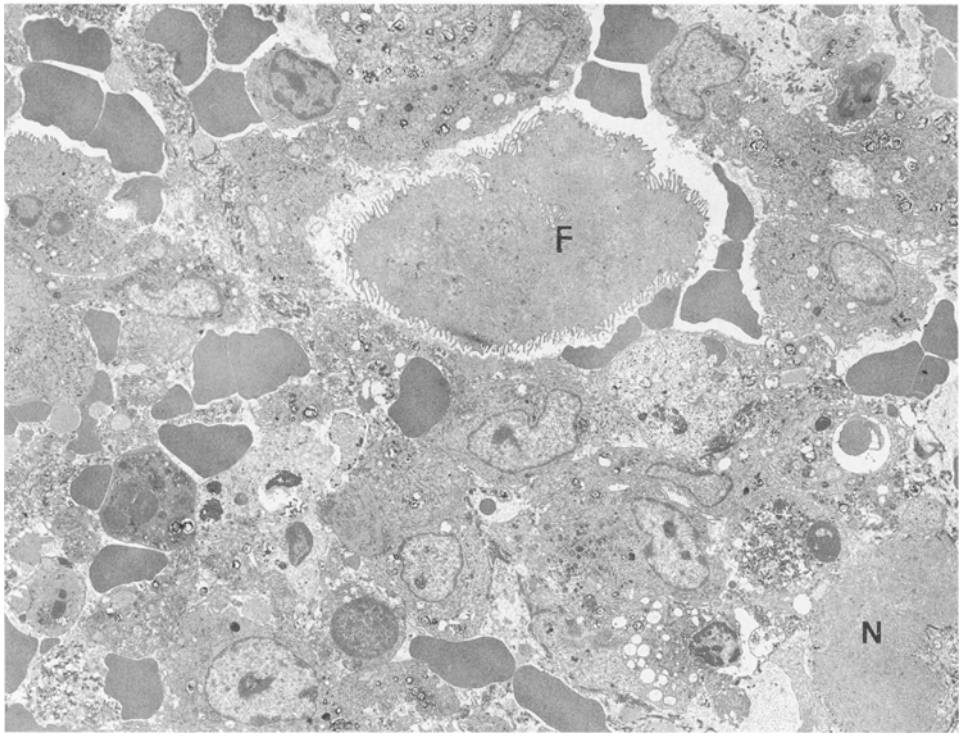

Fig. 6. A filamentous tumour cell (*F*) and a nodular amyloid deposit (*N*) are noted. The filamentous tumour cell is shrunken and detached from the neighbouring tumour cells

amyloid deposits and had deep cytoplasmic invaginations, where closely packed amyloid fibrils were arrayed in parallel fashion (Fig. 9). Membrane-bounded amyloid fibrils were observed in the cytoplasm of a few tumour cells (Fig. 10).

Macrophages were scattered among tumour cells and amyloid deposits, but there were no intimate relationships between amyloid deposits and macrophages.

The results of immunohistochemical staining and the ultrastructural findings are summarized in Table 1.

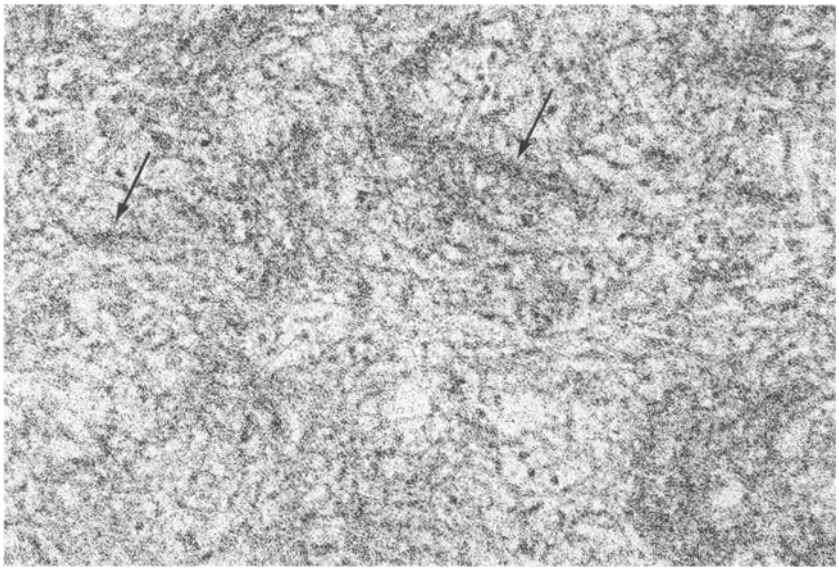

Fig. 7. Electron-dense fibrils (*arrows*), 10–30 nm in width, are intermingled with amyloid fibrils in a nodular amyloid deposit. ×100000

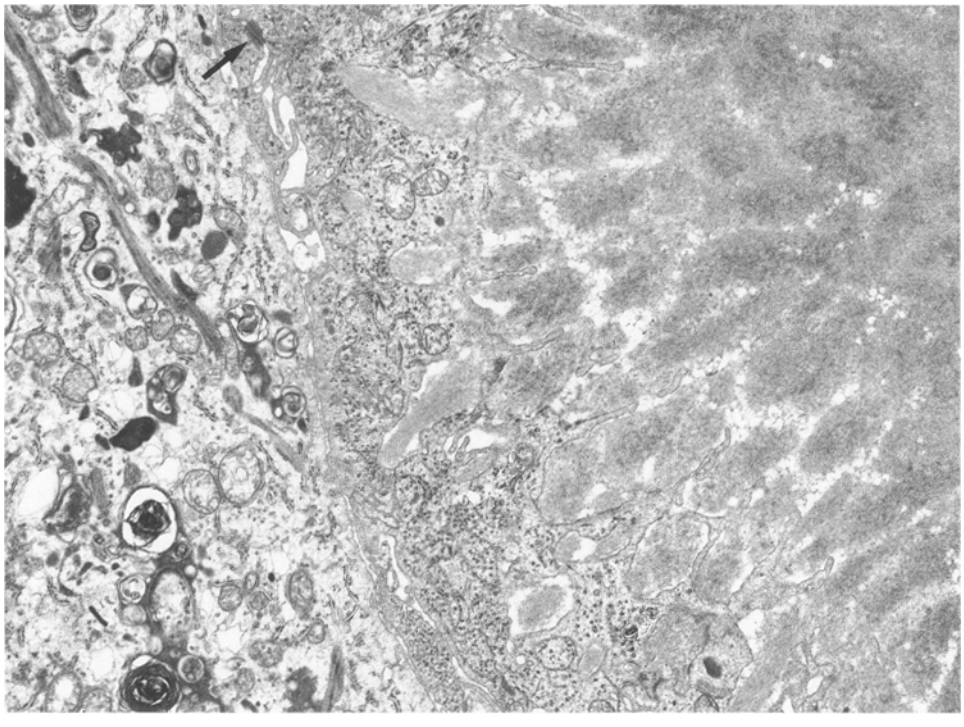

Fig. 8. Amyloid bundles consisting a star-like amyloid deposit are observed adjacent to a tumour cell. The tumour cell has a desmosome (*arrow*). ×10000

Discussion

The amyloid deposits in this study reacted only with an anti-keratin antiserum. Ultrastructurally two forms, nodular and star-like amyloid deposits, were observed. Nodular amyloid deposits were ultrastructurally identical to those described in primary localized cutaneous amyloidosis (Hashimoto and Kumakiri 1979; Kumakiri and Hashimoto 1979). Filamentous tumour cells and filamentous masses were observed together with the amyloid deposits, findings which suggest that nodular amyloid deposits are derived from the tumour cells through filamentous degeneration.

The star-like amyloid deposits are one of the most characteristic features of this study. The tumour cells had deep cytoplasmic invaginations in the vicinity of the amyloid bundles. In addition, membrane-bounded amyloid fibrils were demonstrated in the cytoplasm of the tumour cells. These findings have not been reported in localized amyloidosis related to keratin but, in localized amyloidosis of endocrine origin, similar findings have been reported (Mori et al. 1985; Yamashita et al.

Fig. 9. Amyloid fibrils in deep cytoplasmic invaginations are arrayed in parallel fashion. ×40000

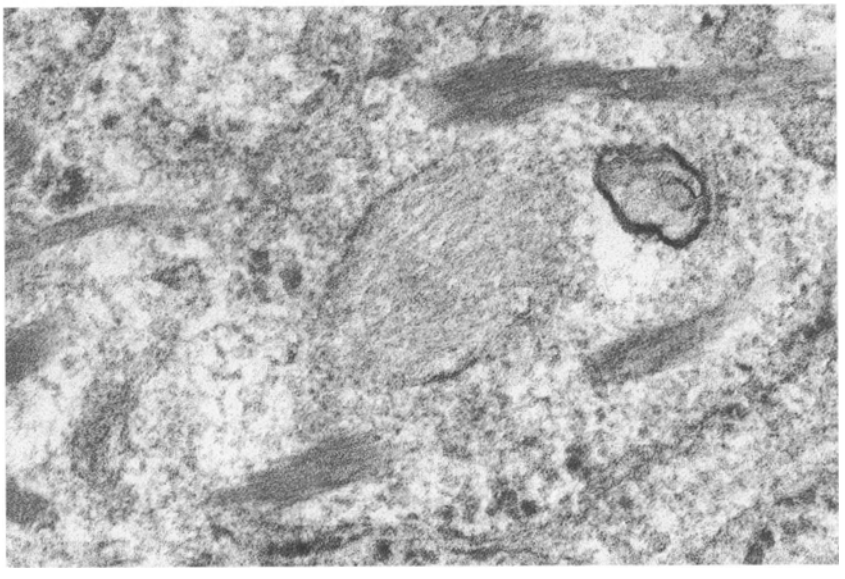

Fig. 10. Membrane-bounded amyloid fibrils locate close to tonofilaments. ×80000

Table 1. Results of immunohistochemical stainings and ultrastructural findings

	Immunohistochemistry					Ultrastructure
	Aκ	Aλ	AA	TTR	Ker	
Case 1	–	–	–	–	–/+ [a]	NA and SA
Case 2	–	–	–	–	–	NA and FD
Case 3	–	–	–	–	–	NA, FD and SA
Case 4	–	–	–	–	–	NA, FD and SA

[a] Positive in frozen section
TTR, Transthyretin; Ker, keratin; NA, nodular amyloid deposits; FD, filamentous degeneration; SA, star-like amyloid deposits

1985; Takahashi et al. 1986). Amyloid fibrils directly transformed from beta granules in secretory vesicles have been observed in the beta cells in a case of type III glycogenosis (Takahashi et al. 1986). Reticuloendothelial cells have similar cytoplasmic invaginations in the vicinity of newly formed amyloid fibrils in experimental murine amyloidosis (Uchino 1967; Uchino et al. 1985). We believe that amyloid fibrils in the star-like amyloid deposits are formed within the cytoplasm or in the vicinity of invaginated cytoplasmic membranes of the tumour cells. However, further examination, using an immunoelectron microscopic technique, is necessary to elucidate the pathogenesis on the star-like amyloid deposits.

References

Fujihara S, Balow JE, Costa JC, Glenner GG (1980) Identification and classification of amyloid in formalin-fixed, paraffin-embedded tissue sections by the unlabeled immunoperoxidase method. Lab Invest 43:358–365

Hashimoto K (1976) Apoptosis in lichen planus and several other dermatoses. Intra-epidermal cell death with filamentous degeneration. Acta Derm Venereol (Stockh) 56:187–210

Hashimoto K, Kumakiri M (1979) Colloid-amyloid bodies in PUVA-treated human psoriatic patients. J Invest Dermatol 72:70–80

Hsueh S, Kuo T (1986) Amyloid in squamous cell carcinoma of the vagina: immunohistochemical study with monoclonal antikeratin antibodies. Int J Gynecol Pathol 5:357–361

Kobayashi H, Hashimoto K (1983) Amyloidogenesis in organ-limited cutaneous amyloidosis: an antigenic identity between epidermal keratin and skin amyloid. J Invest Dermatol 80:66–72

Kumakiri M, Hashimoto K (1979) Histogenesis of primary localized cutaneous amyloidosis: sequential change of epidermal keratinocytes to amyloid via filamentous degeneration. J Invest Dermatol 73:150–152

Looi LM (1983) Localized amyloidosis in basal cell carcinoma. Cancer 52:1833–1836

Malak JA, Smith EW (1962) Secondary localized cutaneous amyloidosis. Arch Dermatol 86:125–137

Masu S, Hosokawa M, Seiji M (1981) Amyloid in localized cutaneous amyloidosis: immunofluorescence studies with anti-keratin antiserum especially concerning the difference between systemic and localized cutaneous amyloidosis. Acta Derm Venereol (Stockh) 61:381–384

Meyer JS (1968) Fine structure of two amyloid-forming medullary carcinomas of thyroid. Cancer 21:406–425

Mori H, Mori S, Saitoh Y, Iida S, Matsumoto K (1985) Growth-hormone-producing pituitary adenoma with crystal-like amyloid immunohistochemically positive for growth hormone. Cancer 55:96–102

Prathap K, Looi LM, Prasad U (1984) Localized amyloidosis in nasopharyngeal carcinoma. Histopathology 8:27–34

Schober R, Nelson D (1975) Fine structure and origin of amyloid deposits in pituitary adenoma. Arch Pathol 99:403–410

Takahashi M, Yokota T, Ishihara T, Uchino F, Kamei T (1986) Insular amyloid in a case of type III glycogenosis with a special reference to the origin of amyloid fibrils. Ultrastruct Pathol 10:235–240

Uchino F (1967) Pathological study on amyloidosis. Role of reticuloendothelial cells in inducing amyloidosis. Acta Pathol Jpn 17:49–82

Uchino F, Takahashi M, Yokota T, Ishihara T (1985) Experimental amyloidosis. Role of the hepatocytes and Kupffer cells in amyloid formation. Appl Pathol 3:78–87

Westermark P, Grimelius L (1973) The pancreatic islet cells in insular amyloidosis in human diabetic and non-diabetic adults. Acta Pathol Microbiol Scand [A] 81:291–300

Yamashita Y, Okuzono Y, Yokota T, Takahashi M, Ishihara T, Uchino F, Kamei T, Adachi H, Iwata T, Matsumoto N, Hirai S, Hatao K, Kaku K, Kaneko T (1985) Morphologic study of three cases of insulinoma. Histochemical and ultrastructural studies. Cancer 55:841–847